

Memory effects in repeated uses of quantum channels

Hayden Zammit ,¹ Roberto Benjamin Salazar Vargas ,¹ Gianluca Valentino ,² Johann A. Briffa ,² and Tony J. G. Apollaro ,¹

¹*Department of Physics, University of Malta, Msida MSD 2080, Malta*

²*Department of Communications and Computer Engineering, University of Malta, Msida MSD 2080, Malta*
(Dated: November 11, 2025)

Quantum Information Processing (QIP) tasks can be efficiently formulated in terms of quantum dynamical maps, whose formalism is able to provide the appropriate mathematical representation of the evolution of open quantum systems. A key QIP task is quantum state transfer (QST) aimed at sharing quantum information between distant nodes of a quantum network, enabling, e.g. quantum key distribution and distributed quantum computing. QST has primarily been addressed insofar by resetting the quantum channel after each use, thus giving rise to memoryless channels. Here we consider the case where the quantum channel is continuously used, without implementing time- and resource-consuming resetting operations. We derive a general, analytical expression for the n^{th} -use average QST fidelity for $U(1)$ -symmetric channels and apply our formalism to a perfect QST channel in the presence of imperfect readout timing. We show that even relatively small readout timing errors give rise to memory effects which have a highly detrimental impact on subsequent QST tasks.

I. INTRODUCTION

Quantum Information Processing (QIP) generally requires a precise sequence of perfectly timed and controlled operations. Control of qubit interactions for quantum gate operations [1] and accurate synchronization of input–output procedures such as state preparation and readout [2] are key for the successful implementation of a QIP protocol. Despite remarkable progress in time-controlled operations, both experimental imperfections and fundamental limits on timekeeping precision [3] prevent perfect temporal control. Consequently, even minor timing mismatches can induce significant errors in the performance of QIP tasks, motivating extensive research on the impact of timing errors [4] and on the energetic cost of achieving high temporal accuracy [5]. In this work, we combine these two perspectives by investigating how many times a quantum channel can be sequentially used to perform a fundamental QIP task, the quantum state transfer (QST) of a single qubit, before an energetic cost needs to be spent in order to reset it to its initial state because of detrimental memory effects [6, 7].

Although single-use QST is well studied [8–11], repeated-use scenarios remain poorly understood due to memory effects generated across uses. Understanding how such effects alters the channel’s dynamics and information capacity is vital for scalable quantum networks, making memory-full channels a central focus of current research [12]. Their proper characterization is essential for enhancing signal throughput in optical fibers [13] and mitigating cross-talk noise in solid-state quantum processors [14]. While the impact of memory effects has been widely explored in optical systems [15–17], they remain largely uncharted in solid-state based channels. Notably, Ref. [18], analyzed a four-site Heisenberg spin- $\frac{1}{2}$ chain that under two successive uses demonstrated that memory effects can enhance both classical and quantum capacities compared to the memoryless case. Similarly,

Ref. [19], proposed a QST protocol that remains reliable in the limit of many uses, provided that the information from the sender qubit is distributed among multiple receivers. These approaches, together with the present work, belong to the class of perfect memory channels [20, 21].

The paper is organized as follows: in Sec. II we develop a general analytical framework for the dynamics of quantum channels used repeatedly without resetting; in Sec. III we apply our formalism to spin- $\frac{1}{2}$ quantum channels with $U(1)$ symmetry, obtaining an exact expression for the n^{th} -use average fidelity; in Sec. IV we focus on a perfect state transfer (PST) spin- $\frac{1}{2}$ model determining the impact of memory effects on the QST quality and providing an upper bound on the quantum channel capacity; finally, in Sec. V we draw our conclusions.

II. MODEL

We consider the following protocol for the transfer of the information from a sender register to a receiver register as illustrated in Fig. 1:

1. The channel is initialized in $|\Psi\rangle_{C_1} = |000\dots000\rangle$. At time $t_0 = 0$, the 1st qubit of the sender register, in an arbitrary state $|\Psi\rangle_{S_1} = \cos \frac{\theta_1}{2} |0\rangle + \sin \frac{\theta_1}{2} e^{i\phi_1} |1\rangle$, and of the receiver register, in the state $|0\rangle_{R_1}$, are attached to the channel;
2. The system $S + C + R$ evolves for a time t_1 , when the 1st sender and receiver qubits are substituted with the 2nd set, respectively in the states $|\Psi\rangle_{S_2} = \cos \frac{\theta_2}{2} |0\rangle + \sin \frac{\theta_2}{2} e^{i\phi_2} |1\rangle$ and $|0\rangle_{R_2}$. The whole system is then let to evolve for a time t_2 .
3. This procedure is repeated until the whole sender register is transferred to the receiver register.

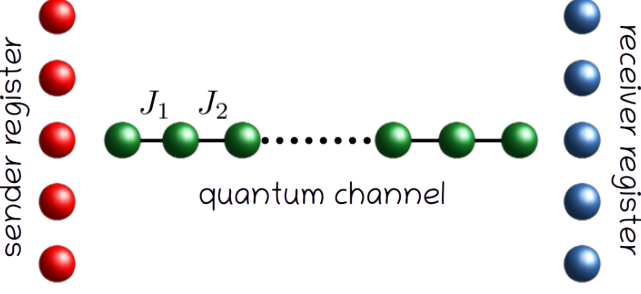


FIG. 1. A quantum channel (green spheres) for the transfer of quantum information between two quantum registers: a sender register (red spheres) and a receiver register (blue spheres).

Our figure of merit is the average n^{th} -use QST fidelity without resetting the quantum channel to $|\Psi\rangle_{C_1}$. We define the n^{th} -use average fidelity:

$$\langle F_n(t_n; t_1) \rangle = \int d\psi \langle \Psi |_{S_n} \hat{\rho}_R^{(n)}(t_n; t_1) | \Psi \rangle_{S_n}, \quad (1)$$

where the state of the n^{th} -use receiver is given by

$$\begin{aligned} \hat{\rho}_R^{(n)}(t_n; t_1) &= \underset{S, C}{\text{Tr}} [\hat{\rho}_{SRC}(t_n; t_1)] \\ &= \underset{S, C}{\text{Tr}} \left[\hat{U}(t_n) \hat{\rho}_S^{(n)} \hat{\rho}_C^{(n-1)}(t_{n-1}; t_1) \hat{\rho}_R^{(n)} \hat{U}^\dagger(t_n) \right], \end{aligned} \quad (2)$$

and the state of the channel is given by the output of the previous use

$$\begin{aligned} \hat{\rho}_C^{(n-1)}(t_{n-1}; t_1) &= \underset{S, R}{\text{Tr}} [\hat{\rho}_{SRC}(t_{n-1}; t_1)] \\ &= \int d\psi \underset{S, R}{\text{Tr}} \left[\hat{U}(t_{n-1}) \hat{\rho}_S^{(n-1)} \hat{\rho}_C^{(n-2)}(t_{n-2}; t_1) \hat{\rho}_R^{(n-1)} \hat{U}^\dagger(t_{n-1}) \right] \end{aligned} \quad (3)$$

where $(t_{n-1}; t_1) \equiv (t_{n-1}, t_{n-2}, \dots, t_2, t_1)$. The integration is done over the Bloch sphere with respect to the normalized Haar measure, which accounts for the standard scenario where the sender states of previous channel uses are unknown.

III. RESULTS

Our main result is the following exact expression for the n^{th} -use average fidelity in eq. (1) for $U(1)$ -symmetric quantum channels, i.e., when $[\hat{H}, \hat{M}_z] = 0$, when \hat{H} can be mapped to quadratic fermion models:

$$\langle F_n(t_n; t_1) \rangle = \frac{1}{2} + \frac{|f_1^N(t_n)| A_{n-1}(t_{n-1}; t_1)}{3} + \frac{|f_1^N(t_n)|^2}{6}, \quad (4)$$

where $f_i^j(t_k) = \langle j | \hat{U}(t_k) | i \rangle$ are transition amplitudes and $A_{n-1}(t_{n-1}; t_1)$ accounts for the memory effects acquired during each use. Eq. 4 is derived from the average n^{th} -use fidelity of general $U(1)$ -symmetric quantum

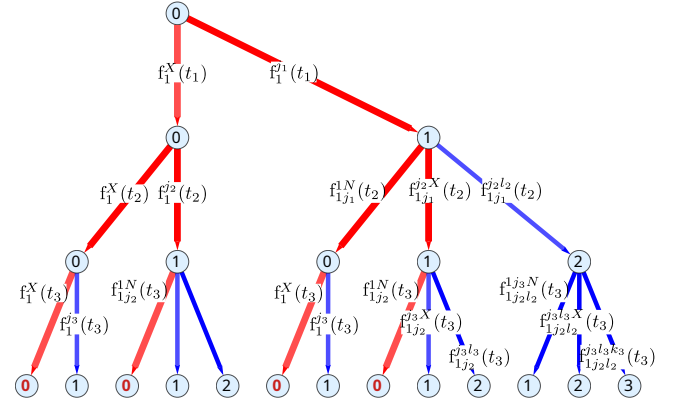


FIG. 2. Mixed-degree rooted tree showing the transition amplitudes entering the term $A_{n-1}(t_{n-1}; t_1)$ in eq. (4). The relevant transition amplitudes are along the Motzkin paths marked in red. Each vertex (blue dot) shows the number of excitations inside the channel after the readout procedure. The edges represent transition amplitudes between the states with the number of excitations between connected vertices.

channels given in eq. (17) in the Appendix. Notably, the structure of the n^{th} -use average fidelity is independent of the number of uses n and equals the structure of the 1st-use expression in Ref. [8].

The memory effects, encoded into $A_{n-1}(t_{n-1}; t_1)$, are determined by summing over all the paths in the mixed-degree rooted tree graph in Fig. 2 that end in 0 and multiplying all the transition amplitudes at times $(t_{n-1}; t_1)$. The graph is constructed by labeling each node with integers $n \geq 0$ and applying the generation rule

$$G(n) = \begin{cases} \{0, 1\} & n = 0 \\ \{n-1, n, n+1\} & n > 0 \end{cases} \quad (5)$$

at each readout time t_i . Using the graph in Fig. 2, it is straightforward to determine the n^{th} -use average fidelity. As an illustrative case, we derive the memory effect for the 4th-use. The term $A_3(t_3, t_2, t_1)$ in eq. (4) is obtained as the sum of the four Motzkin [22] paths:

$$\begin{aligned} &\bullet 0000 \rightarrow \prod_{i=1}^3 \sum_{X_i \in \{1, N\}} |f_1^{X_i}(t_i)|^2 \\ &\bullet 0100 \rightarrow \left| \sum_{j_1 \in C} f_1^{j_1}(t_1) f_{1j_1}^{1N}(t_2) \right|^2 \sum_{X \in \{1, N\}} |f_1^X(t_3)|^2 \\ &\bullet 0010 \rightarrow \sum_{X \in \{1, N\}} |f_1^X(t_1)|^2 \left| \sum_{j_2 \in C} f_1^{j_2}(t_2) f_{1j_2}^{1N}(t_3) \right|^2 \\ &\bullet 0110 \rightarrow \sum_{X \in \{1, N\}} \left| \sum_{j_1, j_2 \in C} f_1^{j_1}(t_1) f_{1j_1}^{j_2 X}(t_2) f_{1j_2}^{1N}(t_3) \right|^2 \end{aligned}$$

The quadratic property of the Hamiltonian can then be utilized to further reduce eq. (4) in terms of only single-particle transition amplitudes [23] using Slater determinants. For instance, the product of single- and two-particle transition amplitudes appearing in the 0100 Motzkin path transforms as follows into products of single-particle amplitudes

$$\sum_{j_1 \in C} f_1^{j_1}(t_1) f_{1j_1}^{1N}(t_2) = \sum_{j_1 \in C} f_1^{j_1}(t_1) \begin{vmatrix} f_1^1(t_2) & f_1^N(t_2) \\ f_{j_1}^1(t_2) & f_{j_1}^N(t_2) \end{vmatrix} \quad (6)$$

Furthermore, exploiting the completeness relation $\sum_{i=1}^N |i\rangle\langle i| = \mathbb{1}$, the sum over the channel's spins can be eliminated. The term arising by expanding the determinant in eq. (6) can be expressed in terms of transition amplitudes involving only the sender and the receiver,

$$\begin{aligned} \sum_{j_1 \in C} f_{j_1}^N(t_2) f_1^{j_1}(t_1) &= \sum_{j_1 \in C} \langle N | \hat{U}(t_2) | j_1 \rangle \langle j_1 | \hat{U}(t_1) | 1 \rangle \\ &= \langle N | \hat{U}(t_2) (\mathbb{1} - |1\rangle\langle 1| - |N\rangle\langle N|) \hat{U}(t_1) | 1 \rangle \quad (7) \\ &= f_1^N(t_1 + t_2) - f_1^1(t_1) f_1^N(t_2) - f_1^N(t_1) f_N^N(t_2) \\ &:= B_1^N(t_2, t_1) = B_2 \end{aligned}$$

Notably, the procedure outlined in eq. (7) entails that the n^{th} -use average fidelity can be determined, in spin- $\frac{1}{2}$ Hamiltonians that map to free fermion models [24], just by means of the transition amplitudes involving the sender and the receiver. This finding constitutes our second main result.

To showcase the usability and the convenience of our approach for repeated uses of a quantum channel for QST, let us report a few n^{th} -use scenarios. Clearly, our result coincides with the first-use average fidelity $\langle F_1(t) \rangle$ given in Ref. [8]

$$\langle F_1(t_1) \rangle = \frac{1}{2} + \frac{|f_1^N(t_1)|}{3} + \frac{|f_1^N(t_1)|^2}{6}, \quad (8)$$

as there is no Motzkin path at the top of the graph in Fig. 2 where $A_0(t_0) = 1$. The 2nd-use average fidelity reads

$$\langle F_2(t_2, t_1) \rangle = \frac{1}{2} + \frac{|f_1^N(t_2)| A_1(t_1)}{3} + \frac{|f_1^N(t_2)|^2}{6}, \quad (9)$$

with $A_1(t_1) = |f_1^1(t_1)|^2 + |f_1^N(t_1)|^2$, and the 3rd-use average fidelity

$$\langle F_3(t_3, t_2, t_1) \rangle = \frac{1}{2} + \frac{1}{3} |f_1^N(t_3)| A_2(t_2, t_1) + \frac{|f_1^N(t_3)|^2}{6}, \quad (10)$$

where

$$\begin{aligned} A_2(t_2, t_1) &= \left(|f_1^1(t_1)|^2 + |f_1^N(t_1)|^2 \right) \left(|f_1^1(t_2)|^2 + |f_1^N(t_2)|^2 \right) \\ &+ |f_1^N(t_2)| (f_1^1(t_1 + t_2) - f_1^1(t_1) f_N^N(t_2)) \\ &- f_1^1(t_2) (f_1^N(t_1 + t_2) - f_1^N(t_1) f_N^N(t_2))^2. \end{aligned} \quad (11)$$

Higher n^{th} -uses can be similarly expressed and it is evident that the memory effects arising from previous uses, embodied in $A_{n-1}(t_{n-1}; t_1)$ can only be detrimental on the average fidelity for equal readout timing protocols, i.e., $t_n = t_{n-1} = \dots = t_1$, as $0 \leq A_{n-1} \leq A_{n-2} \dots \leq A_1 \leq 1$. The left equality holds when all previous uses have resulted in the excitation being trapped with unit probability inside the channel at previous reading times $\{t_i\}$, whereas the right equality holds when all the excitations have been extracted from the chain successfully at previous reading times. Indeed, the latter scenario corresponds to an effective resetting of the quantum channel.

IV. PST CHAIN

Here we consider spin- $\frac{1}{2}$ chains able to perform PST. Several instances have been proposed based on engineered nearest-neighbor couplings [25, 26] and next-nearest neighbor couplings [27] in the XX Hamiltonian. We focus on the coupling scheme of Ref. [25] where the PST time is $\tau = \frac{\pi}{2}$. The Hamiltonian reads

$$\hat{H} = \sum_{i=1}^{N-1} J_i (\hat{\sigma}_i^x \hat{\sigma}_{i+1}^x + \hat{\sigma}_i^y \hat{\sigma}_{i+1}^y), \quad (12)$$

where $J_i = \sqrt{i(N-i)}$. Experimental realizations of PST with the model in eq. (12) have been realized in superconducting qubits [28] and optical waveguides [29]. The Hamiltonian in eq. (12) maps to a free fermion model and, hence, only single-particle transition amplitudes involving the edge sites enter the n^{th} -use average fidelity. Furthermore, these allow an explicit representation in terms of reduced Wigner d -function [30], yielding $f_1^1(t) = f_N^N(t) = (\cos t)^{N-1}$ and $f_1^N(t) = f_N^1(t) = (-i \sin t)^{N-1}$. With these expressions at hand, we can now predict the sequence of QST fidelity for an arbitrary readout timing sequence $\{t_n, t_{n-1}, \dots, t_2, t_1\}$ using eq. (4) and its simplified forms valid for free fermion models as given, e.g. in eqs. (9) and (10). As an illustrative example, let us consider the case where the readout time is affected by a constant shift δ from the ideal PST time τ for all t_i .

In Fig. 3 we see that already for $\delta = 5\%$, the average fidelity reduces to about 0.91 after 10 uses. . Next we consider the n^{th} -use fidelity scaling with the length of the quantum channel. In Fig. 4, we report the value of the average fidelity up to the 5th-use for chain lengths up to $N = 7500$ for a readout error of $\delta = 1\%$. We see that longer chains are more sensitive to readout timing errors, e.g. for a chain of $N = 2150$, already the 4th-use yields a fidelity that is attainable by Local Operations and Classical Communications (LOCC) [31, 32].

Finally, we consider the case where the quantum channel is used to distribute entanglement. The formalism developed for QST can be readily applied for entanglement distribution exploiting the quantum dynamical map formalism [33, 34]: $\hat{\rho}_{ij}^{(s'r)} = \Phi_{ij}^{nm}(t) \hat{\rho}_{nm}^{(s's)}$, with

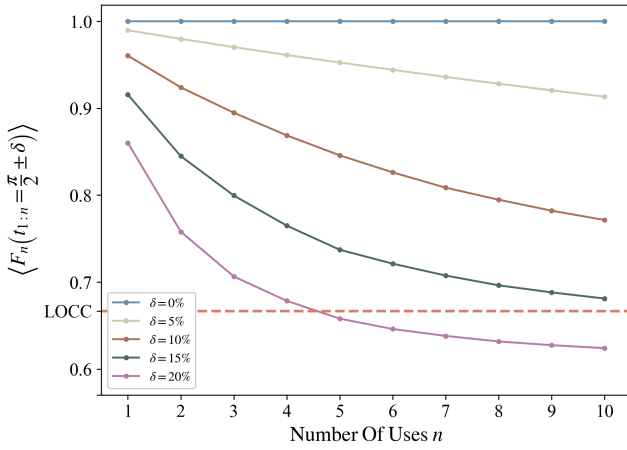


FIG. 3. Average n^{th} -use fidelity for a chain of fixed length $N = 6$ in eq. (12) for different readout timing errors δ . The red dashed line reports the LOCC limit $\frac{2}{3}$. Apart from the ideal scenario of $\delta = 0\%$, each subsequent use of the quantum channel lowers the fidelity.

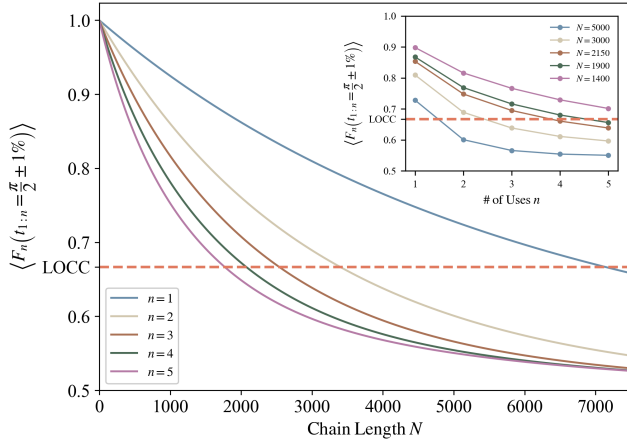


FIG. 4. Average fidelity for a fixed readout timing error of $\delta = 1\%$ for different chain lengths in eq. (12). Each curve represents a different number of uses $n = 1, 2, \dots, 5$. Already after a few uses, chains in the order of 10^3 sites fall below the LOCC limit (red dashed line). The inset shows the average n^{th} -use fidelity along vertical lines of the main plot for selected lengths N .

$i, j, n, m = 0, 1, 2, 3$. The map, acting on the qubits $(s's)$ and producing the output of the qubits $(s'r)$, is obtained by $\Phi^{(s's)}(t) = \mathbb{1}^{(s')} \otimes \Lambda^{(s)}$, with $\Lambda^{(s)}$ denoting the single-qubit map acting on the sender. Whereas the first use of the quantum channel Φ_1 results in the standard amplitude damping channel [35], we directly derive the following expression for the 2nd-use dynamical map as the product of two completely positive trace-preserving (CPTP) maps:

$$\Phi_2 = \Phi_{\text{GAD}}(\gamma_2, p_2) \Phi_{\text{PD}}(\lambda_2) \quad (13)$$

where Φ_{GAD} and Φ_{PD} are the superoperators corresponding respectively to a generalized amplitude damping and a dephasing channel [36–38].

In the computational basis they read,

$$\Phi_{\text{GAD}}(\gamma_2, p_2) = \begin{pmatrix} 1 - \frac{1}{2}|B_2|^2 & 0 & 0 & 1 - \frac{1}{2}|B_2|^2 - |f_1^N(t_2)|^2 \\ 0 & f_1^N(t_2)^* & 0 & 0 \\ 0 & 0 & f_1^N(t_2) & 0 \\ \frac{1}{2}|B_2|^2 & 0 & 0 & \frac{1}{2}|B_2|^2 + |f_1^N(t_2)|^2 \end{pmatrix} \quad (14)$$

and

$$\Phi_{\text{PD}}(\lambda_2) = \begin{pmatrix} 1 & 0 & 0 & 0 \\ 0 & A_1(t_1) & 0 & 0 \\ 0 & 0 & A_1(t_1) & 0 \\ 0 & 0 & 0 & 1 \end{pmatrix} \quad (15)$$

with damping parameter $\gamma_2 = 1 - |f_1^N(t_2)|^2$, mixing probability $p_2 = \frac{1}{\gamma_2} [1 - \frac{1}{2}|B_2|^2 - |f_1^N(t_2)|^2]$, and dephasing $\lambda_2 = 1 - (A_1(t_1))^2$.

Employing the bottleneck inequality [39] over eq. (13), and then exploiting the convexity of the quantum channel capacity $Q(\cdot)$ for degradable channels [36, 39], the following bound for the quantum capacity of the 2nd-use channel is straightforward:

$$Q(\Phi_2) \leq p_2 I_c[\Phi_{\text{AD}}(\gamma_2, 0)] + (1 - p_2) I_c[\Phi_{\text{AD}}(\gamma_2, 1)] \quad (16)$$

for any $\gamma_2 < 1/2$ and where the channel coherent information $I_c[\Phi] = \max_{\rho_s \in \mathcal{B}(\mathcal{H}_s)} \{I_c(\rho_s, \Phi)\}$ stands for the maximum over input states of the standard coherent information [40, 41]. For channel uses at equal time intervals $t_2 = t_1$, since $Q(\Phi_1) = I_c[\Phi_{\text{AD}}(\gamma_2, 1)] = I_c[\Phi_{\text{AD}}(\gamma_2, 0)]$ [36], the upper bound in eq. (16) guarantees that $Q(\Phi_2) \leq Q(\Phi_1)$ for any $\gamma_2 = \gamma_1 = 1 - |f_1^N(t_1)|^2 < 1/2$ and from the bottleneck inequality we have $Q(\Phi_2) = Q(\Phi_{\text{AD}}(\gamma_2, p)) = 0$ for $\gamma_2 = \gamma_1 \geq 1/2$ due to antidegradability of Φ_{AD} [36]. Hence, the second use of the channel reduces its ability to transmit quantum information for any protocol, establishing a limitation on the efficiency of entanglement distribution through repeated uses in uniform intervals. We illustrate the above by implementing the protocol of Ref. [8], where entanglement initially shared by the qubit pair (s', s) is transferred to (s', r) . As shown in Fig. 5, the first use yields finite concurrence [42] for all times $t \neq 0$ or π , while when $t_2 = t_1$ the second use exhibits broad time windows of vanishing entanglement transfer, exposing the destructive role of channel memory.

V. CONCLUSIONS

We have investigated an analytic framework for evaluating memory effects on the QST average fidelity and on the distributed entanglement due to repeated uses of a $U(1)$ -symmetric quantum channel. We obtained

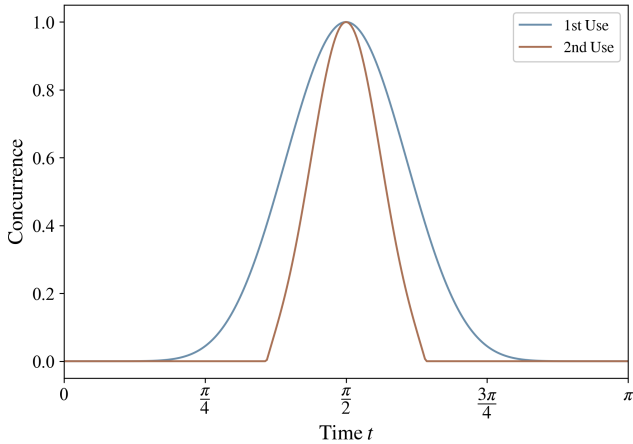


FIG. 5. Entanglement distribution for the 1st- (blue curve) and 2nd-use (red curve) across the quantum channel modeled by eq. (12) with $N = 10$ as a function of time. Whereas the 1st-use admits a non-zero concurrence between s' and r at any $t \neq 0$ or π , the 2nd-use admits only a reduced time-window for entanglement distribution.

an exact expression of the average fidelity for an arbitrary number of uses of the quantum channel in terms of single-particle transition amplitudes involving only the sender and receiver sites when the quantum channel is represented by a quadratic Hamiltonian in its fermionic

representation. We showed that the average fidelity becomes increasingly sensitive to readout timing errors with the number of uses and, interestingly, commonly investigated entanglement distribution protocols, e.g. based on the PST quantum channel, may be inefficient already after the first use in the presence of unavoidable readout timing errors. Our results are readily applicable to a variety of quantum state and entanglement distribution protocols [43–47] and may have an important role in discriminating which one is more robust in terms of multiple uses, contributing thus both to the scalability and the energy efficiency of quantum technologies where QST and entanglement distribution are key primitives.

VI. ACKNOWLEDGEMENTS

HZ and TJGA are grateful to Karol Zyczkowski for useful discussions. The authors acknowledge funding by Xjenza Malta under the grant agreement n. DTP-2024-13 (ATTESTER).

VII. APPENDIX

In the case of a $U(1)$ -symmetric Hamiltonian that is not quadratic in the fermionic representation, the n^{th} -use average fidelity is given by

$$\langle F_n(t_n; t_1) \rangle = \frac{1}{2} + \frac{1}{3} \left| \left[\sum_{k=0}^{\min\{n-1, N\}} \sum_{p_{[k]}, q_{[k]}} \sum_{p'_{[k]}} \rho_{p_{[k]}, q_{[k]}}^{(n-1)}(t_{n-1}; t_1) f_{1p_{[k]}}^{p'_{[k]}N}(t_n) f_{q_{[k]}}^{p'_{[k]}}(t_n)^* \right] \right| + \frac{1}{6} \left[\sum_{k=0}^{\min\{n-1, N\}} \sum_{p_{[k]}, q_{[k]}} \rho_{p_{[k]}, q_{[k]}}^{(n-1)}(t_{n-1}; t_1) \left(\sum_{p'_{[k]}} f_{p_{[k]}}^{p'_{[k]}}(t_n) f_{q_{[k]}}^{p'_{[k]}}(t_n)^* - \sum_{p'_{[k+1]}} f_{1p_{[k]}}^{p'_{[k+1]}}(t_n) f_{1q_{[k]}}^{p'_{[k+1]}}(t_n)^* \right) \right] \quad (17)$$

where $p_{[k]}$ and $q_{[k]}$ refer to length k sets of indices over the chain excluding the sender and receiver sites, whereas sets $p'_{[k]}$ also include the sender site. The $\rho_{p_{[k]}, q_{[k]}}^{(n-1)}$ refer

to the density channel elements of the k^{th} particle sector of the previous use. Finally, the summation over k runs up to $n-1$ while the chain is unsaturated, after which $n-1$ is replaced with its maximum value N .

[1] C. P. Koch, U. Boscain, T. Calarco, G. Dirr, S. Filipp, S. J. Glaser, R. Kosloff, S. Montangero, T. Schulte-Herbrüggen, D. Sugny, and F. K. Wilhelm, Quantum optimal control in quantum technologies. Strategic report on current status, visions and goals for research in Europe, EPJ Quantum Technology **9**, 10.1140/epjqt/s40507-022-00138-x (2022), arXiv:2205.12110.

[2] L. Robledo, L. Childress, H. Bernien, B. Hensen, P. F. A.

Alkemade, and R. Hanson, High-fidelity projective readout of a solid-state spin quantum register, Nature **477**, 574 (2011).

[3] F. Meier, E. Schwarzhans, P. Erker, and M. Huber, Fundamental accuracy-resolution trade-off for timekeeping devices, Physical Review Letters **131**, 220201 (2023), arXiv:2301.05173 [quant-ph].

[4] J. Xuereb, P. Erker, F. Meier, M. T. Mitchison, and M. Huber, Impact of Imperfect Timekeeping on Quantum

Control, Physical Review Letters **131**, 160204 (2023).

[5] F. Meier, Y. Minoguchi, S. Sundelin, T. J. G. Apollaro, P. Erker, S. Gasparinetti, and M. Huber, Precision is not limited by the second law of thermodynamics, Nature Physics **21**, 1147 (2025).

[6] M. Navascués, Resetting Uncontrolled Quantum Systems, Physical Review X **8**, 031008 (2018).

[7] L. Bassman Oftelie, A. De Pasquale, and M. Campisi, Dynamic Cooling on Contemporary Quantum Computers, PRX Quantum **5**, 030309 (2024).

[8] S. Bose, Quantum communication through an unmodulated spin chain, Phys. Rev. Lett. **91**, 207901 (2003).

[9] G. M. Nikolopoulos and I. Jex, *Quantum State Transfer and Network Engineering*, edited by G. M. Nikolopoulos and I. Jex (Springer Berlin Heidelberg, Berlin, Heidelberg, 2014).

[10] L. Banchi, G. Coutinho, C. Godsil, and S. Severini, Pretty good state transfer in qubit chains—the heisenberg hamiltonian, Journal of Mathematical Physics **58**, 032202 (2017).

[11] T. J. G. Apollaro, S. Lorenzo, F. Plastina, M. Consiglio, and K. Życzkowski, Entangled States Are Harder to Transfer than Product States, Entropy **25**, 46 (2022), arXiv:2301.04443.

[12] F. Caruso, Quantum channels and memory effects, Reviews of Modern Physics **86**, 1203 (2014).

[13] F. A. Mele, G. D. Palma, M. Fanizza, V. Giovannetti, and L. Lami, Optical fibers with memory effects and their quantum communication capacities, IEEE Transactions on Information Theory **70**, 8844 (2024).

[14] M. Sarovar, T. Proctor, K. Rudinger, K. Young, E. Nielsen, and R. Blume-Kohout, Detecting crosstalk errors in quantum information processors, Quantum **4**, 321 (2020).

[15] G. Benenti, A. D’Arrigo, and G. Falci, Enhancement of Transmission Rates in Quantum Memory Channels with Damping, Physical Review Letters **103**, 020502 (2009).

[16] F. Caruso, V. Giovannetti, and G. M. Palma, Teleportation-Induced Correlated Quantum Channels, Physical Review Letters **104**, 020503 (2010).

[17] F. A. Mele, L. Lami, and V. Giovannetti, Restoring Quantum Communication Efficiency over High Loss Optical Fibers, Physical Review Letters **129**, 180501 (2022).

[18] A. Bayat, D. Burgarth, S. Mancini, and S. Bose, Memory effects in spin-chain channels for information transmission, Physical Review A **77**, 050306 (2008).

[19] V. Giovannetti, D. Burgarth, and S. Mancini, Communication through a quantum link, Phys. Rev. A **79**, 012311 (2009).

[20] G. Bowen and S. Mancini, Quantum channels with a finite memory, Phys. Rev. A **69**, 012306 (2004).

[21] V. Giovannetti, A dynamical model for quantum memory channels, Journal of Physics A: Mathematical and General **38**, 10989 (2005).

[22] R. Donaghey and L. W. Shapiro, Motzkin numbers, Journal of Combinatorial Theory, Series A **23**, 291 (1977).

[23] T. J. G. Apollaro, S. Lorenzo, F. Plastina, M. Consiglio, and K. Życzkowski, Quantum transfer of interacting qubits, New Journal of Physics **24**, 083025 (2022), arXiv:2205.01579.

[24] E. Lieb, T. Schultz, and D. Mattis, Two soluble models of an antiferromagnetic chain, Annals of Physics **16**, 407 (1961).

[25] M. Christandl, N. Datta, A. Ekert, and A. J. Landahl, Perfect State Transfer in Quantum Spin Networks, Physical Review Letters **92**, 187902 (2004).

[26] L. Vinet and A. Zhedanov, How to construct spin chains with perfect state transfer, Physical Review A **85**, 012323 (2012).

[27] M. Christandl, L. Vinet, and A. Zhedanov, Analytic next-to-nearest-neighbor XX models with perfect state transfer and fractional revival, Physical Review A **96**, 032335 (2017).

[28] X. Li, Y. Ma, J. Han, T. Chen, Y. Xu, W. Cai, H. Wang, Y. P. Song, Z. Y. Xue, Z. Q. Yin, and L. Sun, Perfect Quantum State Transfer in a Superconducting Qubit Chain with Parametrically Tunable Couplings, Physical Review Applied **10**, 1 (2018), arXiv:1806.03886.

[29] R. J. Chapman, M. Santandrea, Z. Huang, G. Corrielli, A. Crespi, M.-H. Yung, R. Osellame, and A. Peruzzo, Experimental perfect state transfer of an entangled photonic qubit, Nature Communications **7**, 11339 (2016).

[30] M. Christandl, N. Datta, T. C. Dorlas, A. Ekert, A. Kay, and A. J. Landahl, Perfect transfer of arbitrary states in quantum spin networks, Physical Review A **71**, 032312 (2005).

[31] R. Horodecki, P. Horodecki, M. Horodecki, and K. Horodecki, Quantum entanglement, Reviews of Modern Physics **81**, 865 (2009).

[32] E. Chitambar, D. Leung, L. Mančinska, M. Ozols, and A. Winter, Everything you always wanted to know about locc (but were afraid to ask), Communications in Mathematical Physics **328**, 891 (2014).

[33] I. Bengtsson and K. Życzkowski, *Geometry of Quantum States* (Cambridge University Press, Cambridge, 2017).

[34] S. Lorenzo, F. Plastina, M. Consiglio, and T. J. G. Apollaro, Quantum Map Approach to Entanglement Transfer and Generation in Spin Chains (2022) pp. 321–340, arXiv:2112.02348.

[35] S. Bose, Quantum communication through spin chain dynamics: an introductory overview, Contemporary Physics **48**, 13 (2007), <https://doi.org/10.1080/00107510701342313>.

[36] S. Khatri, K. Sharma, and M. M. Wilde, Information-theoretic aspects of the generalized amplitude-damping channel, Phys. Rev. A **102**, 012401 (2020).

[37] I. Devetak and P. W. Shor, The capacity of a quantum channel for simultaneous transmission of classical and quantum information, Communications in Mathematical Physics **256**, 287 (2005).

[38] Z. Puchała, K. Korzekwa, R. Salazar, P. Horodecki, and K. Życzkowski, Dephasing superchannels, Phys. Rev. A **104**, 052611 (2021).

[39] M. M. Wolf and D. Pérez-García, Quantum capacities of channels with small environment, Phys. Rev. A **75**, 012303 (2007).

[40] H. Barnum, M. A. Nielsen, and B. Schumacher, Information transmission through a noisy quantum channel, Phys. Rev. A **57**, 4153 (1998).

[41] M. A. Nielsen and I. L. Chuang, *Quantum Computation and Quantum Information*, 10th ed. (Cambridge University Press, Cambridge, 2010).

[42] W. K. Wootters, Entanglement of formation of an arbitrary state of two qubits, Physical Review Letters **80**, 2245 (1998), arXiv:quant-ph/9709029.

[43] A. Kay, Perfect state transfer: Beyond nearest-neighbor

couplings, *Physical Review A - Atomic, Molecular, and Optical Physics* **73**, 1 (2006).

[44] T. J. G. Apollaro, L. Banchi, A. Cuccoli, R. Vaia, and P. Verrucchi, 99 % -fidelity ballistic quantum-state transfer through long uniform channels, *Physical Review A* **85**, 052319 (2012).

[45] R. Ronke, M. P. Estarellas, I. D'Amico, T. P. Spiller, and T. Miyadera, Anderson localisation in spin chains for perfect state transfer, *The European Physical Journal D* **70**, 189 (2016).

[46] J. Zhou, M. Li, W. Wang, W. Cai, Z. Hua, Y. Xu, X. Pan, G. Xue, H. Zhang, Y. Song, H. Yu, C.-L. Zou, and L. Sun, Quantum State Transfer between Superconducting Cavities via Exchange-Free Interactions, *Physical Review Letters* **133**, 220801 (2024).

[47] M. Junior, G. Almeida, and F. De Moura, Quantum state transfer in ladder systems with cross-correlated disorder, *Physica E: Low-dimensional Systems and Nanostructures* **171**, 116249 (2025).